Computing and Visualization in Science manuscript No.
(will be inserted by the editor)

A. Naumovich · F.J. Gaspar

On a multigrid solver for the three-dimensional Biot poroelasticity system in multilayered domains

Received: date / Accepted: date

Abstract In this paper, we present problem–dependent prolongation and problem–dependent restriction for a multigrid solver for the three-dimensional Biot poroelasticity system, which is solved in a multilayered domain. The system is discretized on a staggered grid using the finite volume method. During the discretization, special care is taken of the discontinuous coefficients. For the efficient multigrid solver, a need in operator-dependent restriction and/or prolongation arises. We derive these operators so that they are consistent with the discretization. They account for the discontinuities of the coefficients, as well as for the coupling of the unknowns within the Biot system. A set of numerical experiments shows necessity of use of the operator-dependent restriction and prolongation in the multigrid solver for the considered class of problems.

1 Introduction

Biot poroelasticity system describes a number of processes modeled by flows in deformable porous media, which are of interest for geoscience, bioscience and engineering. This system first appeared within the phenomenological theory of consolidation [3], and later on it was re-derived via homogenization theory. Existence and uniqueness of the solution of the system are analyzed in [11].

Most of the works in this area treat the case of continuous coefficients. However, often natural porous media (soil, rock, skin), as well as manufactured one (filtering media, paper, textile, etc.), have layered structures with layers characterized by different porosity, permeability, etc. To model the deformation and flow processes within such media, a need to consider Biot model with discontinuous coefficients appears.

Analytical solution of Biot system is available only in very special cases, and therefore, numerical methods are commonly used for solving the respective initial-boundary value problem. Finite element method is preferred in many cases especially when dealing with complex domains or adaptive grids. However, often solutions generated by finite element methods as well as by finite difference method on collocated grids exhibit nonphysical oscillations. To avoid this, finite difference discretization on staggered grid has been suggested and theoretically analyzed in [6].

The problem is more complicated when the coefficients have discontinuities along material interfaces, e.g. for the multilayered porous media, especially when it is essential to capture accurately the solution near the interface. Finite volume methods are known to produce an accurate discretization for PDEs and systems of PDEs with discontinuous coefficients. The discrete schemes obtained after such a discretization are conservative - they preserve the fluxes across the interfaces of discontinuities, and such schemes ensure higher accuracy for stresses and fluxes near the interfaces. These two features are very important for many practical applications.

In our paper, we deal with the finite volume discretization on the staggered grids, what allows us to derive stable and accurate discretization for the Biot system with strongly discontinuous coefficients. To solve

This research has been partially supported by the Kaiserslautern Excellence Cluster Dependable Adaptive Systems and Mathematical Modelling, the Spanish project MEC/FEDER MTM 2004-019051, the Diputacin General de Aragn, and by the INTAS project 03-50-4395.

A. Naumovich
Fraunhofer Institut Techno- und Wirtschaftsmathematik
Fraunhofer-Platz 1
D-67663 Kaiserslautern.
Tel.: +49-0631-31600 4692
Fax: +49-0631-31600 5692
E-mail: naumovic@itwm.fhg.de

F.J. Gaspar
Departamento de Matemática Aplicada. University of Zaragoza.
Maria de Luna 3, 50018 Zaragoza Spain.
Tel.: +34-976-762010
Fax: +34-976-761886
E-mail: fjgaspar@unizar.es

efficiently the system of linear equations, produced by the finite volume discretization, the multigrid method is applied. Remind, that since we are solving a system of PDEs with discontinuous coefficients, efficient multigrid solver for this problem should account for discontinuous coefficients as well as for the coupling of the unknowns within the system of PDEs.

The development of efficient multigrid methods for systems of PDEs requires special attention. Extensions of the multigrid methods developed for a scalar PDE are required, for some recent achievements we refer to, [8], [4], [5] and references therein. On the other hand, special multigrid techniques are also required to solve efficiently linear systems arising after discretization of scalar PDEs or systems of PDEs with discontinuous coefficients. A basic approach in such cases is to derive and apply problem–dependent prolongation and/or restriction operators, see, e.g., [1], [14], [9]. Up to authors best knowledge, there was no discussion in the literature on problem–dependent intergrid operators for the poroelasticity system, and this paper aims at filling this gap. The multigrid solver presented here is an extension of the one discussed in [13], [7], where the case of homogeneous porous medium is treated, i.e. Biot system with continuous coefficients is considered there.

The remainder of the paper is organized as follows. Biot poroelasticity system, and the respective finite volume discretization of the problem are presented in Section 2. Section 3, which is the most important one, is devoted to the construction of the multigrid solver for the interface problem considered here. Some numerical results are presented in Section 4, and some conclusions are drawn at the end.

2 Mathematical model and finite volume discretization

2.1 Continuous system

Classical Biot model [3,2] describes consolidation of linearly elastic porous solid. This model can be formulated as a system of PDEs for the unknowns fluid pressure $p(\mathbf{x},t)$ and displacement of the porous medium $\mathbf{u} = \mathbf{u}(\mathbf{x},t) = (u,v,w)$

$$-\left((\lambda+2\mu)u_x + \lambda\left(v_y+w_z\right)\right)_x - \left(\mu\left(u_y+v_x\right)\right)_y - \left(\mu\left(u_z+w_x\right)\right)_z + p_x = 0, \quad (1)$$

$$-\left(\mu\left(v_x+u_y\right)\right)_x - \left((\lambda+2\mu)v_y + \lambda\left(w_z+u_x\right)\right)_y - \left(\mu\left(v_z+w_y\right)\right)_z + p_y = 0, \quad (2)$$

$$-\left(\mu\left(w_x+u_z\right)\right)_x - \left(\mu\left(w_y+v_z\right)\right)_y - \left((\lambda+2\mu)w_z + \lambda\left(u_x+v_y\right)\right)_z + p_z = 0, \quad (3)$$

$$\left(\phi\beta p + u_x + v_y + w_z\right)_t - \left(\kappa p_x\right)_x - \left(\kappa p_y\right)_y - \left(\kappa p_z\right)_z = f(\mathbf{x},t). \quad (4)$$

Here λ and μ are the Lame coefficients of the porous medium, ϕ is the porosity, β is the compressibility of the fluid, κ is the permeability of the porous medium divided by the viscosity of the fluid, and $f(\mathbf{x},t)$ is a source term, which describers, e.g., injection or extraction process.

In this paper, we restrict ourself to the case of the parallelepiped domain $0 \le x \le l_1$, $0 \le y \le l_2$, $0 \le z \le l_3$. Necessary boundary as well as initial conditions should supplement the model.

Layered porous medium results in the discontinuous coefficients of the system (1) - (4) across certain interfaces. Let us consider such an interface $z = \xi$. Then, coefficients of the model are discontinuous across $z = \xi$, and we assume them to be piecewise - constant:

$$\lambda(\mathbf{x}) = \begin{cases} \lambda_1 & \text{for } z < \xi, \\ \lambda_2 & \text{for } z > \xi, \end{cases} \quad \mu(\mathbf{x}) = \begin{cases} \mu_1 & \text{for } z < \xi, \\ \mu_2 & \text{for } z > \xi, \end{cases} \quad (5)$$

$$\kappa(\mathbf{x}) = \begin{cases} \kappa_1 & \text{for } z < \xi, \\ \kappa_2 & \text{for } z > \xi, \end{cases} \quad \phi(\mathbf{x}) = \begin{cases} \phi_1 & \text{for } z < \xi, \\ \phi_2 & \text{for } z > \xi. \end{cases} \quad (6)$$

The following interface conditions should complete the model (1) - (4) to take into account the discontinuities of the coefficients

$$[u] = 0,\ [v] = 0, [w] = 0, [p] = 0, [\kappa p_z] = 0, \quad (7)$$

$$[\mu\left(w_x+u_z\right)] = 0, [\mu\left(w_y+v_z\right)] = 0, \quad (8)$$

$$[(\lambda+2\mu)w_z + \lambda\left(u_x+v_y\right)] = 0. \quad (9)$$

2.2 Finite volume discretization

To overcome stability difficulties, which often arise when the discretization of the Biot model is done on the collocated grids, the use of staggered grids was proposed in [6], [7]. Pressure points of this grid are located on the physical boundary, and displacement points are defined at the respective cell faces. In the three-dimensional case staggered grid is composed of the four following types of the grid points

$$G^u = \{(x_{i+0.5}, y_j, z_k) = ((i+0.5)h_x, jh_y, kh_z),\ i = 0,..,N_1-1,\ j = 0,..,N_2,\ k = 0,..,N_3\},$$

$$G^v = \{(x_i, y_{j+0.5}, z_k) = (ih_x, (j+0.5)h_y, kh_z),\ i = 0,..,N_1,\ j = 0,..,N_2-1,\ k = 0,..,N_3\},$$

$$G^w = \{(x_i, y_j, z_{k+0.5}) = (ih_x, jh_y, (k+0.5)h_z),\ i = 0,..,N_1,\ j = 0,..,N_2,\ k = 0,..,N_3-1\},$$

$$G^p = \{(x_i, y_j, z_k) = (ih_x, jh_y, kh_z),\ i = 0,..,N_1,\ j = 0,..,N_2,\ k = 0,..,N_3\},$$

where N_1, N_2, N_3 are some integers, and $h_x = l_1/N_1$, $h_y = l_2/N_2$, and $h_z = l_3/N_3$ are grid step sizes in the respective directions.

It is well known, that finite volume method can provide an accurate discretization for the PDEs with discontinuous coefficients in a natural way. Accurate discretization concerns primary variables as well as so-called fluxes of the problem. By fluxes of the Biot system we mean fluid flux vector and stress tensor of the porous medium. Since for us these quantities are of a big interest, finite volume method is a natural choice for our problem.

Within the finite volume method, we allow interface to cut control volumes, or, in other words, we do not require alignment of the grid lines with the interface between the media.

Let us suppose that k_{int}, $0 \le k_{int} < N_3$ is such an index that interface position can be represented in the following way

$$\xi = z_{k_{int}} + \theta h_z = k_{int} h_z + \theta h_z, \quad (10)$$

where $0 \le \theta < 1$ is some parameter, which indicates respective location of the interface between the coordinates $z_{k_{int}}$ and $z_{k_{int}+1}$.

For the time discretization we introduce a grid in time with a step-size τ

$$G^t = \{t_n : \ t_n = n\tau, \ n = 0, 1, \ldots, M\}. \quad (11)$$

We also introduce the following grid functions:

$$u = u^n_{i+0.5,j,k} = u_{i+0.5,j,k} = u(x_{i+0.5}, y_j, z_k, t_n),$$
$$v = v^n_{i,j+0.5,k} = v_{i,j+0.5,k} = v(x_i, y_{j+0.5}, z_k, t_n),$$
$$w = w^n_{i,j,k+0.5} = w_{i,j,k+0.5} = w(x_i, y_j, z_{k+0.5}, t_n),$$
$$p = p^n_{i,j,k} = p_{i,j,k} = p(x_i, y_j, z_k, t_n),$$

which are defined on the grids $G^u \times G^t$, $G^v \times G^t$, $G^w \times G^t$, and $G^p \times G^t$ respectively.

Finite volume discretization of the system (1) - (4), (7) - (9) in space and weighted discretization in time results in the following system of discrete equations:

$$\begin{aligned}
&-\big(\langle\lambda+2\mu\rangle^u_{i,j,k} u_{\bar{x},i+0.5,j,k} + \langle\lambda\rangle^v_{i,j,k} v_{\bar{y},i,j+0.5,k} \\
&+ \langle\lambda\rangle^w_{i,j,k} w_{\bar{z},i,j,k+0.5}\big)_x \\
&-\big(\mu_{i+0.5,j-0.5,k}(u_{\bar{y},i+0.5,j,k} + v_{\bar{x},i+1,j-0.5,k})\big)_y \\
&-\big(\langle\mu\rangle^{uw}_{i+0.5,j,k-0.5}(u_{\bar{z},i+0.5,j,k} + w_{\bar{x},i+1,j,k-0.5})\big)_z \\
&+p_{\bar{x},i,j,k} = 0,
\end{aligned}$$

$$\begin{aligned}
&-\big(\langle\lambda+2\mu\rangle^v_{i,j,k} v_{\bar{y},i,j+0.5,k} + \langle\lambda\rangle^u_{i,j,k} u_{\bar{x},i+0.5,j,k} \\
&+ \langle\lambda\rangle^w_{i,j,k} w_{\bar{z},i,j,k+0.5}\big)_y \\
&-\big(\mu_{i-0.5,j+0.5,k}(v_{\bar{x},i+1,j+0.5,k} + u_{\bar{y},i-0.5,j+1,k})\big)_x \\
&-\big(\langle\mu\rangle^{vw}_{i,j+0.5,k-0.5}(v_{\bar{z},i,j+0.5,k} + w_{\bar{y},i,j+1,k-0.5})\big)_z \\
&+p_{\bar{y},i,j,k} = 0,
\end{aligned}$$

$$\begin{aligned}
&-\big(\langle\lambda+2\mu\rangle^w_{i,j,k} w_{\bar{z},i,j,k+0.5} + \langle\lambda\rangle^{uv}_{i,j,k}(u_{\bar{x},i+0.5,j,k} \\
&+ v_{\bar{y},i,j+0.5,k})\big)_z - \\
&-\big(\langle\mu\rangle^{uw}_{i-0.5,j,k+0.5}(w_{\bar{x},i,j,k+0.5} + u_{\bar{z},i-0.5,j,k+1})\big)_x \\
&-\big(\langle\mu\rangle^{vw}_{i,j-0.5,k+0.5}(w_{\bar{y},i,j,k+0.5} + v_{\bar{z},i,j-0.5,k+1})\big)_y \\
&+ \ p_{\bar{z},i,j,k} = 0,
\end{aligned}$$

$$\begin{aligned}
&\big(\langle a\rangle_{i,j,k} p_{i,j,k} + u_{x,i-0.5,j,k} + v_{y,i,j-0.5,k} + w_{z,i,j,k-0.5}\big)_t \\
&-\big(\kappa_{i-0.5,j,k} p^\sigma_{\bar{x}}\big)_x - \big(\kappa_{i,j-0.5,k} p^\sigma_{\bar{y}}\big)_y - \big(\langle\kappa\rangle_{i,j,k-0.5} p^\sigma_{\bar{z}}\big)_z \\
&= \langle f\rangle^\sigma_{i,j,k},
\end{aligned}$$

where $\langle\lambda+2\mu\rangle^u$, $\langle\lambda+2\mu\rangle^v$, $\langle\lambda+2\mu\rangle^w$, $\langle\lambda\rangle^u$, $\langle\lambda\rangle^v$, $\langle\lambda\rangle^w$, $\langle\lambda\rangle^{uv}$, $\langle\mu\rangle^{uw}$, $\langle\mu\rangle^{vw}$, $\langle\kappa\rangle$, $\langle a\rangle = \langle\phi\beta\rangle$ are some averaging of the coefficients in the respective grid points, depending on the coefficient θ, and $\langle f\rangle$ is averaged right hand side of the last equation. We want to mension here that the discretization will be presented in more details in a forthcoming paper.

In the formulas above, $p^\sigma = \sigma p^{n+1} + (1-\sigma)p^n$, and also standard designations for the forward and backward finite differences, $u_{x,i+0.5,j,k} = (u_{i+1.5,j,k} - u_{i+0.5,j,k})/h_x$, $u_{\bar{x},i+0.5,j,k} = (u_{i+0.5,j,k} - u_{i-0.5,j,k})/h_x$, etc. (see, e.g. [10]) were used.

Performed numerical experiments showed that derived discrete system gives second order of convergence for primary variables (displacement components and fluid pressure) as well as for the fluxes of the problem (stress tensor components and fluid velocity components) in the maximum norm. Note that this convergence order is not affected by the interface location with respect to the grid lines.

3 Multigrid method

Multigrid methodology allows to construct efficient linear solvers for large class of problems. Important properties of such solvers are that their convergence does not depend on the discretization grid size, and thus the number of arithmetic operations is proportional to the number of unknowns. Multigrid method is based on two principles: smoothing of the error and coarse grid correction.

Suppose we want to solve an elliptic problem $L_h u_h = f_h$, where h corresponds to the grid size.

Two-grid error transformation operator for this problem reads

$$M_{h,2h} = S_h^{n_2}\left(I_h - P_{2h,h} L_{2h}^{-1} R_{h,2h} L_h\right) S_h^{n_1}, \quad (12)$$

where S_h is the iterative relaxation method (smoother), I_h is the identity operator, $P_{2h,h}$ is the prolongation operator from the coarse to the fine grid, $R_{h,2h}$ is the restriction operator from fine to the coarse grid.

Formula (12) represents the following two-grid algorithm: to perform n_1 steps of pre-smoothing S_h on the fine grid, to calculate the residual and restrict it to the coarse grid using restriction operator $R_{h,2h}$, to solve the coarse grid defect equation exactly, to interpolate calculated correction to the fine grid using prolongation operator $P_{2h,h}$, to correct the current fine grid approximation, and to perform n_2 post-smoothing steps on the fine grid.

Note that if instead of inverting L_{2h} in formula (12) coarse grid equation is recursively solved using the two-grid algorithm, resultant algorithm is called multigrid.

In order to construct the multigrid solver for the particular problem, it is very important to choose its components (smoother S_h, inter-grid transfer operators restriction $R_{h,2h}$ and prolongation $P_{2h,h}$, and a coarse grid operator L_{2h}) in such a way that they efficiently interplay with each other.

3.1 Multigrid method for systems of PDEs.

In order to solve efficiently systems of PDEs with a multigrid method, some its extensions are required. But often, the straight-forward generalizations of the multigrid methodology from the scalar equations to systems of PDEs can handle only weakly coupled systems (e.g. so-called variable-based algebraic multigrid), and when the coupling between the unknowns of the system becomes too strong, the solver becomes inefficient.

In case of strongly coupled systems, when the interdependence between different physical unknowns is important, the multigrid solver should take special care of it. The unknowns in the discrete system, corresponding to different physical unknowns and connections between them should carefully be treated within by multigrid solver. Such considerations had lead to the development of so-called point-block approach in the algebraic multigrid (point-based AMG) (see, e.g. [8],[5]), when all the unknowns of the system corresponding to the same grid point are grouped together, and the coefficient matrix of the problem is written in the respective point-block form. This kind of approach allows to generalize the multigrid philosophy from the scalar PDEs to the systems, and can handle strongly coupled systems in an efficient way.

Following generalizations for systems come out from such approaches. First of all, use of collective relaxation, when all unknowns of the system at each single point are relaxed simultaneously. And second, the interpolation and restriction should be done in the block-wise form, exploiting the information about the interconnections between different unknowns.

Our approach is somewhat similar to the point-block approach in AMG, but we look at the problem from the geometric point of view, and apply the so-called geometric multigrid. This choice is reasonable in our case, because we are dealing with the system, arisen after the discretization of the concrete system of PDEs in the parallelepiped domain, and information about the differential problem and about the geometry is available.

3.2 Multigrid method for problems with discontinuous coefficients.

Usually, convergence of a standard multigrid solver deteriorates as the coefficients of the problem experience discontinuities across certain interfaces between subdomains with different physical properties. Moreover, convergence may depend on the order of discontinuity and on the location of the interface with respect to the grid lines. Special techniques are needed to tackle the difficulties, which arise in such problems.

The difficulty comes from the fact that discontinuous coefficients result in the discontinuous partial derivatives of the solution, and the sizes of these discontinuities are of the same order of magnitude. This implies that use of the prolongation operator, which is based on the linear interpolation is not reasonable for such problems, since for non-smooth functions linear interpolation is inexact, and deterioration of the convergence or even divergence of the multigrid solver is usually observed.

Use of operator-dependent inter-grid transfer operators (restriction and prolongation) is a well known remedy for problems with strongly discontinuous coefficients (see, e.g. [12], [1], [14], [9]). The idea during the construction of such operators is to preserve continuity of the fluxes of the problem across the interface.

Since finite volume method allows to derive conservative schemes, which preserve fluxes in a natural way, properly used information from the finite volume discretization allows us to derive the inter-grid transfer operators which are consistent with discretization and are consequently flux-preserving.

3.3 Multigrid components for Biot system with discontinuous coefficients. Operator-dependent restriction and prolongation.

As it was mentioned above, components of the multigrid solver should be adjusted to each particular problem so that they take into account all particular features of the problem and result in an efficient interplay.

Two main specificities of the problem we are solving are: first of all, it is a system of PDEs, and second - it has discontinuous coefficients.

Remind here, that basic components of the multigrid are smoother, restriction and prolongation operators, and a coarse grid operator. For the smoothing procedure we use the altering line Gauss-Seidel relaxation. The choice for the coarse-grid operator is following: discretize the system on the coarse grid or use Galerkin coarse grid operator. We choose the first option, since the finite volume discretization was done for arbitrary interface position location with respect to the grid lines, and discretization on the coarse grid can be done straightforward.

Now we focus our attention on the derivation of the inter-grid transfer operators. The following is important: we should exploit the interface continuity conditions, and we should account for the interdependence of the unknowns, which correspond to the different unknowns of the continuous system. The use of the information from the finite volume discretization allows us to satisfy these two requirements in a natural way. As it was mentioned above, we make the inter-grid transfer operators consistent with the discretization.

During the finite volume discretization, the interpolating polynomials for all basic unknowns of the system were derived in the corresponding sets of control volumes. These polynomials were obtained in such a way that they satisfy interface conditions, and the information about the interdependence of the different unknowns is already taken into account by coefficients of these polynomials. We use these polynomials, built on the coarse grid, to obtain the values of the unknowns in the fine grid points. This procedure gives us formulas for the interpolation, based on which, the prolongation operator is derived.

Note that, in the text below, all unknowns, coefficients, etc. with upper index f are related to the fine grid, and all unknowns, coefficients, etc. with upper index c are related to the coarse grid.

We start from the interpolation of the first displacement component. Interpolation in x and y directions is made in a standard way. But in z-direction more complicated formulas should be used. Below, formulas for interpolation of u in the fine grid points $(x_{i+0.5}, y_{2j+1}, z_{2k+1}) \in G^{u,f}$ are presented.

If $k = k^c_{int}$ and $\theta^c \leq 1/2$ then

$$u^f_{i+0.5,2j+1,2k+1} = \frac{1}{2}\frac{\mu_1}{\langle\mu\rangle} u(x_{i+0.5}, y_{2j+1}, z_{2k}) + \left(1 - \frac{1}{2}\frac{\mu_1}{\langle\mu\rangle}\right) u(x_{i+0.5}, y_{2j+1}, z_{2k+2}) - \frac{1}{2} h^c_z \theta^c \frac{\mu_1 - \mu_2}{\langle\mu\rangle} w^c_{x,\frac{i}{2},j,k};$$

if $k = k^c_{int}$ and $\theta^c > 1/2$ then

$$u^f_{i+0.5,2j+1,2k+1} = \left(1 - \frac{1}{2}\frac{\mu_2}{\langle\mu\rangle}\right) u(x_{i+0.5}, y_{2j+1}, z_{2k}) + \frac{1}{2}\frac{\mu_2}{\langle\mu\rangle} u(x_{i+0.5}, y_{2j+1}, z_{2k+2}) + \frac{1}{2} h^c_z (\theta^c - 1) \frac{\mu_1 - \mu_2}{\langle\mu\rangle} w^c_{x,\frac{i}{2},j,k},$$

where $\langle\mu\rangle = (1 - \theta^c)\mu_1 + \theta^c \mu_2$.

If $k \neq k^c_{int}$ then linear interpolation for $u^f_{i+0.5,2j+1,2k+1}$ is done.

Note that values $u(x_{i+0.5}, y_{2j+1}, z_{2k})$ and $u(x_{i+0.5}, y_{2j+1}, z_{2k+2})$, which are used in the formulas above are found as a result of linear interpolation in x- and y- directions of the values from the coarse grid points.

Interpolation of the v-component is done in a similar way to the interpolation of u.

Since we are dealing with staggered grids, for the w-component there exist two fine grid points between each two coarse grid points on the vertical lines, i.e. between two coarse points $(x_i, y_j, z_{k+0.5}), (x_i, y_j, z_{k+1.5}) \in G^{w,c}$ two fine grid points $(x_{2i}, y_{2j}, z_{2k+0.5})$ and $(x_{2i}, y_{2j}, z_{2k+1.5}) \in G^{w,f}$ are located.

First, we consider points $(x_{2i}, y_{2j}, z_{2k+0.5})$. If $k = k^c_{int} - 1$, and $\theta^c \leq 1/2$ then

$$w^f_{2i,2j,2k+0.5} = \left(1 - \frac{1}{4}\frac{\lambda_2 + 2\mu_2}{\langle\lambda + 2\mu\rangle_1}\right) w^c_{i,j,k+0.5} + \frac{1}{4}\frac{\lambda_2 + 2\mu_2}{\langle\lambda + 2\mu\rangle_1} w^c_{i,j,k+1.5} + \frac{h^c_z}{4}(\theta^c - 0.5)\frac{(\lambda_1 - \lambda_2)}{\langle\lambda + 2\mu\rangle_1}\left(u^c_{x,i-0.5,j,k+1} + v^c_{y,i,j-0.5,k+1}\right);$$

if $k = k^c_{int}$ and $1/2 < \theta^c \leq 3/4$ then

$$w^f_{2i,2j,2k+0.5} = \frac{3}{4}\frac{\lambda_1 + 2\mu_1}{\langle\lambda + 2\mu\rangle_2} w^c_{i,j,k+0.5} + \left(1 - \frac{3}{4}\frac{\lambda_1 + 2\mu_1}{\langle\lambda + 2\mu\rangle_2}\right) w^c_{i,j,k+1} - \frac{3}{4} h^c_z (\theta^c - 0.5)\frac{(\lambda_1 - \lambda_2)}{\langle\lambda + 2\mu\rangle_2}\left(u^c_{x,i-0.5,j,k+1} + v^c_{y,i,j-0.5,k+1}\right);$$

if $k = k^c_{int}$ and $3/4 < \theta^c \leq 1$ then

$$w^f_{2i,2j,2k+0.5} = \left(1 - \frac{1}{4}\frac{\lambda_2 + 2\mu_2}{\langle\lambda + 2\mu\rangle_2}\right) w^c_{i,j,k+0.5} + \frac{1}{4}\frac{\lambda_2 + 2\mu_2}{\langle\lambda + 2\mu\rangle_2} w^c_{i,j,k+1.5} + \frac{h^c_z}{4}(\theta^c - 1.5)\frac{(\lambda_1 - \lambda_2)}{\langle\lambda + 2\mu\rangle_2}\left(u^c_{x,i-0.5,j,k+1} + v^c_{y,i,j-0.5,k+1}\right),$$

where $\langle\lambda + 2\mu\rangle_1 = (1/2 - \theta^c)(\lambda_1 + 2\mu_1) + (1/2 + \theta^c)(\lambda_2 + 2\mu_2)$, and $\langle\lambda + 2\mu\rangle_2 = (3/2 - \theta^c)(\lambda_1 + 2\mu_1) + (\theta^c - 1/2)(\lambda_2 + 2\mu_2)$.

If none of the cases listed above take place, linear interpolation according to the formula

$$w^f_{2i,2j,2k+0.5} = \frac{3}{4} w^c_{i,j,k+0.5} + \frac{1}{4} w^c_{i,j,k+1.5}$$

is used. Interpolation of w in the points $(x_{2i}, y_{2j}, z_{2k+1.5})$ is done in a similar way.

We can suppose that within the Biot system pressure-to-displacement coupling is weaker than couplings between different displacement components, and that it is weak enough to use such operator-dependent prolongation for pressure, which is done separately from the displacement components. Moreover, this kind of interpolation naturally follows from the finite volume discretization. From the polynomials, used during the discretization for the pressure unknowns, we obtain following formulas for the prolongation in the internal grid points in z-direction:
if $k = k^c_{int}$ and $\theta^c \leq 1/2$ then

$$p^f_{2i,2j,2k+1} = \frac{1}{2}\frac{\kappa_1}{\langle\kappa\rangle} p^c_{i,j,k} + \left(1 - \frac{1}{2}\frac{\kappa_1}{\langle\kappa\rangle}\right) p^c_{i,j,k+1};$$

if $k = k^c_{int}$ and $\theta^c > 1/2$ then

$$p^f_{2i,2j,2k+1} = \left(1 - \frac{1}{2}\frac{\kappa_2}{\langle\kappa\rangle}\right) p^c_{i,j,k} + \frac{1}{2}\frac{\kappa_2}{\langle\kappa\rangle} p^c_{i,j,k+1},$$

where notation $\langle\kappa\rangle = (1 - \theta^c)\kappa_1 + \theta^c \kappa_2$ was used. If $k \neq k^c_{int}$ then linear interpolation is applied.

Note that the formulas for the prolongation of the pressure can be considered as a particular case of the operator dependent prolongation, derived, e.g. in [14,9] for the diffusion equation.

According to the formulas for interpolation, introduced above, in order to calculate values of u and v on the fine grid, values of w from the coarse grid are also used, and to calculate w, coarse grid values of u and v are used. This means that the interdependence of the variables of the system was automatically taken into account.

Often, restriction operator is chosen as the (properly scaled) transpose of the operator-dependent prolongation. In our case, in order to prevent the overgrowth of the stencil of the restriction operator, we transpose the prolongation operator and apply additional lumping. This lumping is done in x - direction for the u - component, y - direction for v - component, and z - direction for w - component, and results in the 18-point stencil for each displacement variable in the internal points. This gives, e.g., the following formula for the restriction in the coarse grid point (x_i, y_j, z_k) with index $k = k^c_{int}$ and when $\theta^c < 1/4$

$$
\begin{aligned}
u^c_{i,j,k} &= \frac{1}{8}(u^f_{2i-1,2j-1,2k-1} + u^f_{2i,2j-1,2k-1}) \\
&+\frac{1}{32}(u^f_{2i-1,2j,2k-2} + u^f_{2i-1,2j-2,2k-2} + u^f_{2i,2j,2k-2} \\
&+u^f_{2i,2j-2,2k-2}) + \frac{1}{16}(u^f_{2i-1,2j-2,2k-1} + u^f_{2i-1,2j,2k-1} \\
&+u^f_{2i,2j,2k-1} + u^f_{2i,2j-2,2k-1} + u^f_{2i-1,2j-1,2k-2} \\
&+u^f_{2i,2j-1,2k-2}) + \frac{1}{16}\frac{\mu_1}{\langle\mu\rangle_1}(u^f_{2i-1,2j-1,2k} + u^f_{2i,2j-1,2k}) \\
&+\frac{1}{32}\frac{\mu_1}{\langle\mu\rangle_1}(u^f_{2i-1,2j,2k} + u^f_{2i-1,2j-2,2k} + \\
&u^f_{2i,2j,2k} + u^f_{2i,2j-2,2k}) \\
&+\frac{1}{16}\frac{h^c_x}{h^c_z}\frac{\lambda_1-\lambda_2}{\langle\lambda+2\mu\rangle_1}((\theta^c-1/2)(w^f_{2i-1,2j-1,2k-2} \\
&-w^f_{2i+1,2j-1,2k-2}) + (\theta^c+1/2)(-w^f_{2i-1,2j-1,2k-1} \\
&+w^f_{2i+1,2j-1,2k-1})) \\
&+\frac{(\theta^c-1/2)}{32}\frac{h^c_x}{h^c_z}\frac{\lambda_1-\lambda_2}{\langle\lambda+2\mu\rangle_1}(w^f_{2i-1,2j,2k-2} \\
&-w^f_{2i+1,2j,2k-2} + w^f_{2i-1,2j-2,2k-2} - w^f_{2i+1,2j-2,2k-2}) \\
&+\frac{(\theta^c+1/2)}{32}\frac{h^c_x}{h^c_z}\frac{\lambda_1-\lambda_2}{\langle\lambda+2\mu\rangle_1}(-w^f_{2i-1,2j,2k-1} \\
&+w^f_{2i+1,2j,2k-1} - w^f_{2i-1,2j-2,2k-1} + w^f_{2i+1,2j-2,2k-1}).
\end{aligned}
$$

Similar formulas are valid for the operator-dependent restriction for the other displacement components in the other points neighboring to the interface.

Operator-dependent restriction for the pressure is obtained like transposed prolongation. No need in lumping appears in this situation. Below you can see, e.g., formula for the restriction of pressure values in the internal coarse grid point with index $k = k^c_{int}$ for the case $\theta^c \le 1/2$

$$
\begin{aligned}
p^c_{i,j,k} &= \frac{1}{8}p^f_{2i-1,2j-1,2k-1} + \frac{1}{16}\Big(p^f_{2i-1,2j,2k-1} \\
&+p^f_{2i-1,2j-2,2k-1} + p^f_{2i,2j-1,2k-1} + p^f_{2i-2,2j-1,2k-1} \\
&+p^f_{2i-1,2j-1,2k-2}\Big) + \frac{1}{32}\Big(p^f_{2i,2j,2k-1} + p^f_{2i,2j-2,2k-1} \\
&+p^f_{2i-2,2j,2k-1} + p^f_{2i-2,2j-2,2k-1} + p^f_{2i-1,2j,2k-2} \\
&+p^f_{2i-1,2j-2,2k-2} + p^f_{2i,2j-1,2k-2} + p^f_{2i-2,2j-1,2k-2}\Big) + \\
&\frac{1}{64}\Big(p^f_{2i,2j,2k-2} + p^f_{2i,2j-2,2k-2} + p^f_{2i-2,2j,2k-2} \\
&+p^f_{2i-2,2j-2,2k-2}\Big) + \frac{1}{16}\frac{\kappa_1}{\langle\kappa\rangle}p^f_{2i-1,2j-1,2k} \\
&+\frac{1}{32}\frac{\kappa_1}{\langle\kappa\rangle}\Big(p^f_{2i-1,2j,2k} + p^f_{2i-1,2j-2,2k} + p^f_{2i,2j-1,2k} + \\
&p^f_{2i-2,2j-1,2k}\Big) + \frac{1}{64}\frac{\kappa_1}{\langle\kappa\rangle}\Big(p^f_{2i,2j,2k} + p^f_{2i,2j-2,2k} \\
&+p^f_{2i-2,2j,2k} + p^f_{2i-2,2j-2,2k}\Big).
\end{aligned}
$$

As one can see from the formulas above, derived restrictions and prolongations for our problem satisfy all necessary requirements - they take into account jumps of coefficients, i.e. are operator-dependent and they are specially adapted to treat the couplings of unknowns within the system of PDEs.

4 Numerical experiments

In this article we present two sets of numerical experiments. In the first set of the experiments exact solution of the Biot system is known, and within these experiments we evaluate both convergence of the obtained approximate solution to the known exact solution, as well as the convergence of the multigrid method. In the second set of experiments we consider a physical model, which can be described with the Biot system with discontinuous coefficients. In this case the exact solution is unknown. Within this experiment, we calculate the physical characteristics of the process, and also evaluate the convergence of the multigrid.

In order to see the advantages of the use of the operator-dependent prolongation and/or operator-dependent restriction, in both experiments we performed the following comparison. We considered four multigrid solvers - based on both linear interpolation and restriction (we call this solver $M(P^{lin}, R^{lin})$), based on operator - dependent prolongation and linear restriction ($M(P^{od}, R^{lin})$), based on operator - dependent restriction and linear prolongation ($M(P^{lin}, R^{od})$), and based on both operator - dependent restriction and prolongation ($M(P^{od}, R^{od})$).

Convergence of the multigrid solver was estimated using value of the convergence factor, which we calculate with the following formula

$$\rho^n = \sqrt[n]{\frac{\|r^n\|}{\|r^0\|}},$$

where n is the number of multigrid iterations necessary to achieve given tolerance for the residual, and

$$\|r^n\| = \sum_{i=1,4} \|r_i^n\|,$$

where each of $\|r_i^n\|$ is the maximum norm of the residual of i-th equation of the system after the n-th iteration.

4.1 Example 1.

We choose the exact solution of the continuous problem (1)-(9) to be following:

$$u^{ex}(x,y,z,t) = \begin{cases} \frac{1}{\mu_1}\cos(\pi x) y \sin(z-\xi) e^{-t}, & 0 \le z < \xi, \\ \frac{1}{\mu_2}\cos(\pi x) y \sin(z-\xi) e^{-t}, & \xi < z \le 1, \end{cases}$$

$$v^{ex}(x,y,z,t) = \begin{cases} \frac{1}{\mu_1} x \cos(\pi y) \sin(z-\xi) e^{-t}, & 0 \le z < \xi, \\ \frac{1}{\mu_2} x \cos(\pi y) \sin(z-\xi) e^{-t}, & \xi < z \le 1, \end{cases}$$

$$w^{ex}(x,y,z,t) = \begin{cases} \frac{1}{\lambda_1+2\mu_1} xy \sin(z-\xi) e^{-t}, & 0 \le z < \xi, \\ \frac{1}{\lambda_2+2\mu_2} xy \sin(z-\xi) e^{-t}, & \xi < z \le 1, \end{cases}$$

$$p^{ex}(x,y,z,t) = \begin{cases} \frac{1}{\kappa_1} xy(z-\xi) \sin(z) e^{-t}, & 0 \le z < \xi, \\ \frac{1}{\kappa_2} xy(z-\xi) \sin(z) e^{-t}, & \xi < z \le 1. \end{cases}$$

The boundary conditions in this experiment are calculated from the exact solution and look as following:

Dirichlet boundary condition for the pressure on the entire boundary

$$p(\mathbf{x},t) = p^{ex}(\mathbf{x},t).$$

Neumann or Dirichlet conditions for u, v, w on the corresponding parts of the boundary

$$\frac{\partial u}{\partial x} = \frac{\partial u^{ex}}{\partial x}, \; v = v^{ex}, \; w = w^{ex}, \text{ at } x = 0,1,$$

$$u = u^{ex}, \; \frac{\partial v}{\partial y} = \frac{\partial v^{ex}}{\partial y}, \; w = w^{ex}, \text{ at } y = 0,1,$$

$$u = u^{ex}, \; v = v^{ex}, \; \frac{\partial w}{\partial z} = \frac{\partial w^{ex}}{\partial z}, \text{ at } z = 0,1.$$

Initial conditions are also set from the exact solution

$$\mathbf{u}(\mathbf{x},0) = \mathbf{u}^{ex}(\mathbf{x},0), \; p(\mathbf{x},0) = p^{ex}(\mathbf{x},0).$$

The right-hand sides of all equations are non-zero in this experiment, and their analytical expressions can be found using known exact solutions.

We assign the time discretization parameter $\sigma = 1$, what corresponds to the fully-implicit discretization in time, and we only use one time step. We note that in case of use of several steps in time, the convergence results, calculated on one time layer, are representative for the others. The following values of parameters are chosen for the experiment: $T = 0.1$, $\xi = 0.501$, and $\beta = 0$ (fluid is incompressible). Let the coefficients of the problem λ, μ and κ experience jumps of the seven orders of magnitude, and $\lambda_1 = 1$, $\mu_1 = 1$, $\kappa_1 = 1$, $\lambda_2 = 10^7$, $\mu_2 = 10^7$, $\kappa_2 = 10^7$.

Table 1 Example 1: Convergence factor ρ^n and number of multigrid iterations (in brackets) for the multigrid solvers: 1. $M(P^{lin}, R^{lin})$, 2. $M(P^{od}, R^{lin})$, 3. $M(P^{lin}, R^{od})$, and 4. $M(P^{od}, R^{od})$.

Grid	1.	2.	3.	4.
$8 \times 8 \times 8$	diverges	0.16 (9)	0.13 (8)	0.12 (8)
$16 \times 16 \times 16$	diverges	0.13 (9)	0.12 (8)	0.11 (8)
$32 \times 32 \times 32$	diverges	0.09 (7)	0.09 (7)	0.08 (7)
$64 \times 64 \times 64$	diverges	0.06 (6)	0.07 (7)	0.06 (6)

This problem was solved by the multigrid method. In the numerical experiments F(2,2) multigrid cycle was used, and we remind that the smoother is alternating line Gauss-Seidel.

Comparison of the solvers $M(P^{lin}, R^{lin})$, $M(P^{od}, R^{lin})$, $M(P^{lin}, R^{od})$, and $M(P^{od}, R^{od})$, applied to this problem, was performed. The results of comparison are summarized in Table 1. Note that, in this table, e.g. grid $16 \times 16 \times 16$ means that in the sub-grids of the staggered grid G^u, G^v, G^w, G^p values $N_1 = N_2 = N_3 = 17$. As one can see from the results, it is enough to use only operator-dependent restriction or only operator-dependent prolongation. In the case of both standard (linear) prolongation and restriction, the multigrid solver does not converge (for the comparison of it with $M(R^{od}, P^{od})$ see Fig. 1 and 2).

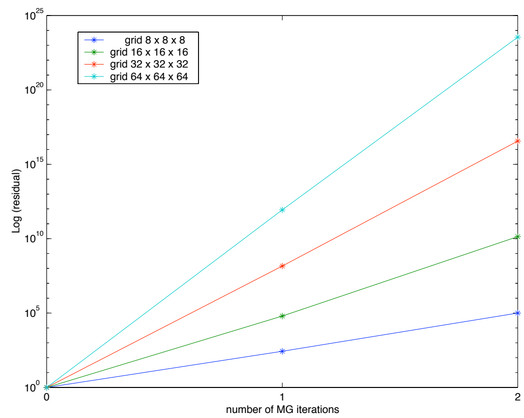

Fig. 1 Example 1: Divergence of the multigrid solver $M(R^{lin}, P^{lin})$.

Note that multigrid solvers $M(P^{od}, R^{lin})$, $M(P^{lin}, R^{od})$, and $M(P^{od}, R^{od})$ are robust with respect to the size of the jumps in the coefficients, but their convergence can slightly vary for the different interface positions.

We should especially note that during the numerical experiments second order convergence in the maximum norm in space was observed for primary variables (dis-

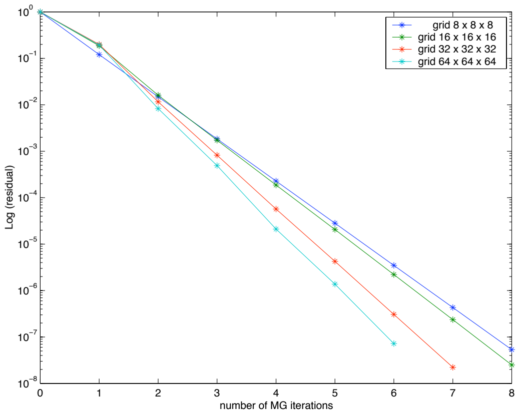

Fig. 2 Example 1: Convergence of the multigrid solver $M(R^{od}, P^{od})$.

placement components and pressure) as well as for the fluxes of the problem.

4.2 Example 2.

Consider the two-layered porous medium saturated with incompressible fluid ($\beta = 0$). Local load is applied on the upper surface of the medium on the square $[x_1; x_2] \times [y_1; y_2]$. The upper and lower surfaces of the medium are free to drain, and lateral walls are rigid and impermeable. As a result of the applied load porous medium is deforming, and fluid flows through the layers.

The following boundary conditions correspond to this situation: on the lower surface ($z = 0$) $\mathbf{S}^n = 0$ and $p = 0$; on the lateral surfaces ($x = 0$ or $x = 1$ or $y = 0$ or $y = 1$) $\mathbf{u} = 0$ and $\mathbf{V}^n = 0$; on the upper surface ($z = 1$) $S^n = \mathbf{S}^{loc}$, if $(x, y) \in [x_1; x_2] \times [y_1; y_2]$, and $\mathbf{S}^n = 0$ otherwise, and $p = 0$. $\mathbf{S}^n$ and $\mathbf{V}^n$ designate here normal stress tensor component and normal fluid velocity component respectively with respect to the corresponding surfaces, and $\mathbf{S}^{loc}$ is the applied load.

We solve this problem in the domain $[0; 1] \times [0; 1] \times [0; 1]$. The following parameters of the porous layers, separated by the interface $\xi = 0.499$ were considered - lower layer: $\lambda_1 = 10^4$, $\mu_1 = 10^4$, $\kappa_1 = 10^{-1}$; upper layer: $\lambda_2 = 1$, $\mu_2 = 1$, $\kappa_2 = 10^{-4}$. As one can see from the parameters, the upper porous layer is more soft, but less permeable than the lower one. The vertical local load of the value 5 is applied on the square $[0.15; 0.25] \times [0.15; 0.25]$. The time interval is $[0; 1]$, and we only use one time step.

This problem was solved by the $F(2, 1)$ - cycle on the different grids. Convergence results are presented in Table 2.

As in the Example 1, multigrid solver based on both standard restriction and prolongation does not converge. The comparison of it with $M(R^{od}, P^{od})$ is shown at Fig. 3 and 4. Some of the calculated physical characteristics of the process (in the corresponding cross-sections) are presented in Figures 5 - 11. The calculations for these figures were done on the grid $32 \times 32 \times 32$.

Figures 5 and 6 show the fluid pressure values in the different cross-sections: the first cross-section crosses the local load and the second one not. It is natural, that values of the fluid pressure are larger directly under the load, than at some distance from it.

In Figures 7 and 8 vertical displacements are shown in the same cross-sections as the fluid pressure. The largest negative values for the vertical displacements are below the load (note that z-axe is oriented upward). Note also that small positive vertical displacement appears in some distance from the load near the upper boundary.

Table 2 Example 2: Convergence factor ρ^n and number of multigrid iterations (in brackets) for the multigrid solvers: 1. $M(P^{lin}, R^{lin})$, 2. $M(P^{od}, R^{lin})$, 3. $M(P^{lin}, R^{od})$, and 4. $M(P^{od}, R^{od})$.

Grid	1.	2.	3.	4.
$16 \times 16 \times 16$	diverges	0.15 (10)	0.21 (10)	0.12 (9)
$32 \times 32 \times 32$	diverges	0.20 (10)	0.23 (10)	0.13 (9)
$64 \times 64 \times 64$	diverges	0.24 (10)	0.32 (10)	0.08 (8)

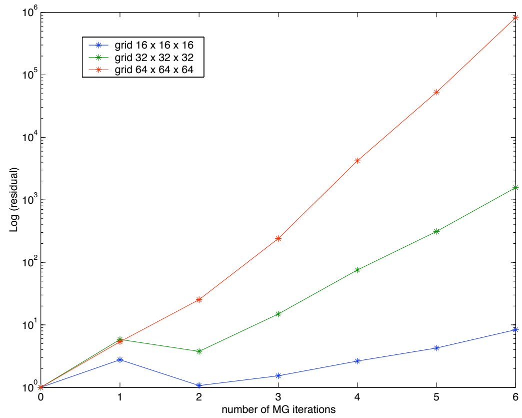

Fig. 3 Example 2: Divergence of the multigrid solver $M(R^{lin}, P^{lin})$.

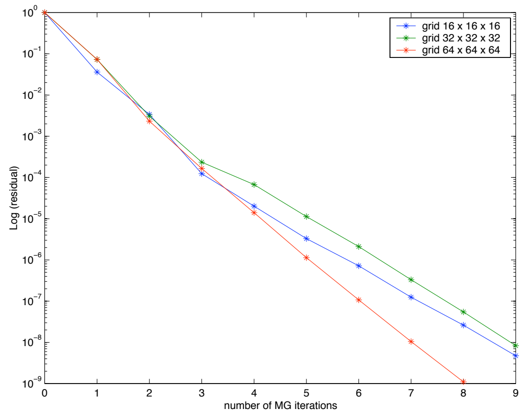

Fig. 4 Example 2: Convergence of the multigrid solver $M(R^{od}, P^{od})$.

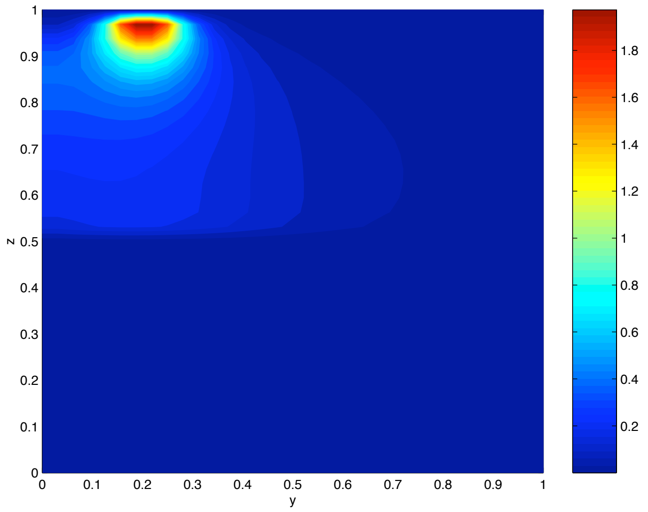

Fig. 5 Example 2: Pressure of the fluid in the cross-section $x = 0.1875$.

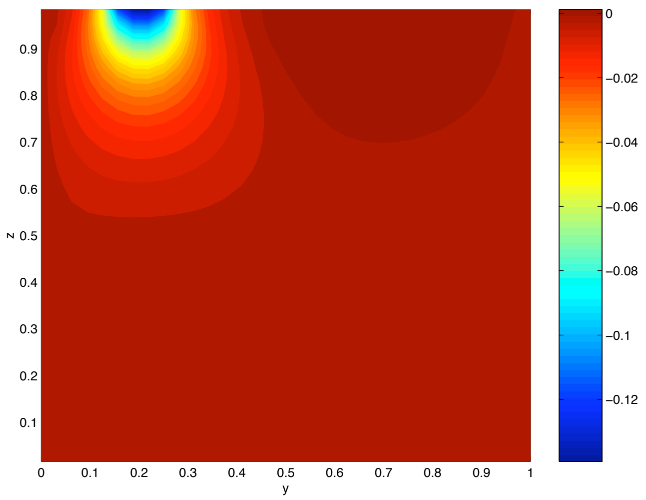

Fig. 7 Example 2: Vertical displacement component in the cross-section $x = 0.1875$.

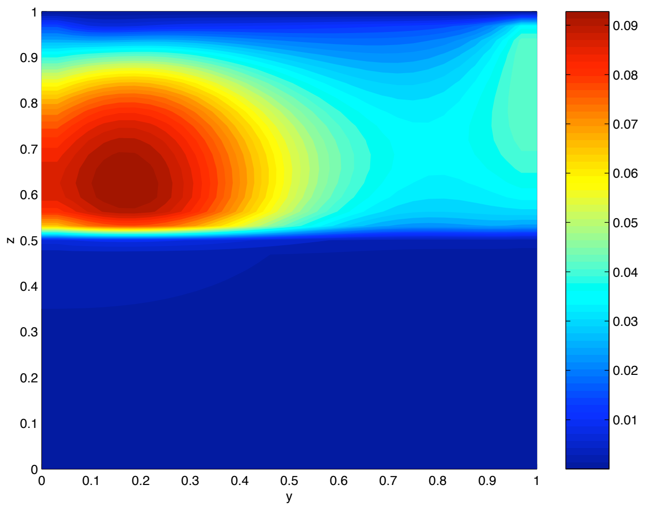

Fig. 6 Example 2: Pressure of the fluid in the cross-section $x = 0.53125$.

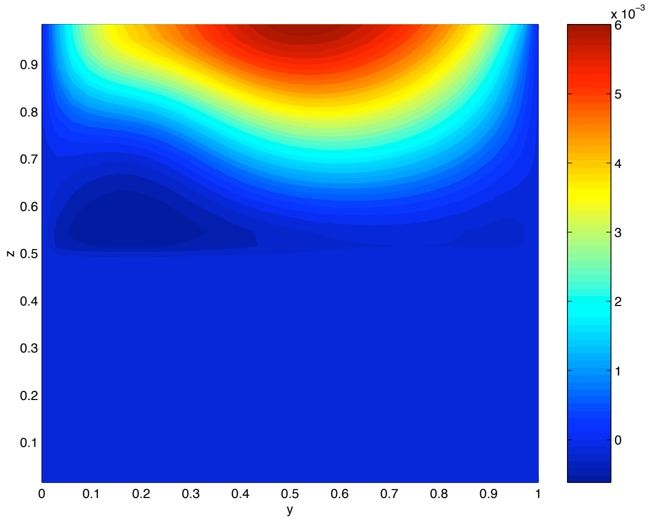

Fig. 8 Example 2: Vertical displacement component in the cross-section $x = 0.53125$.

It is well known that values of the stress tensor components are very important in many real problems. At Figures 9 - 12, the tensor stress component $S^{zz} = (\lambda + 2\mu)\, w_z + \lambda\,(u_x + v_y)$ in different vertical and horizontal cross-sections is shown.

5 Conclusions

In this paper, a multigrid solver for the three-dimensional Biot poroelasticity system in a multilayered domain is derived. The finite volume discretization on a staggered grid is presented. The operator-dependent restriction and prolongation operators are derived consistently with the finite volume discretization. A set of numerical experiments shows advantages of the use of the operator-dependent restriction and prolongation in the multigrid solver for the considered problem.

References

1. R.E. Alcouffe, A. Brandt, J.E. Dendy, Jr. and J.W. Painter, The multi-grid method for the diffusion equation with strongly discontinuous coefficients, *SIAM J.Stat.Comput.* **2**, No.4, 430-454 (1981)
2. J. Bear, Y. Bachmat, Introduction to modeling of transport Phenomena in Porous Media, Kluwer Academic, Dordrecht (1990).
3. M. Biot, General theory of three dimensional consolidation. *J. Appl. Phys.* **12**, 155–164 (1941).
4. T. P. Chartier, Element-based algebraic multigrid (AMGe) and spectral AMGe. *PhD Thesis, Univercity of Colorado* (2001).

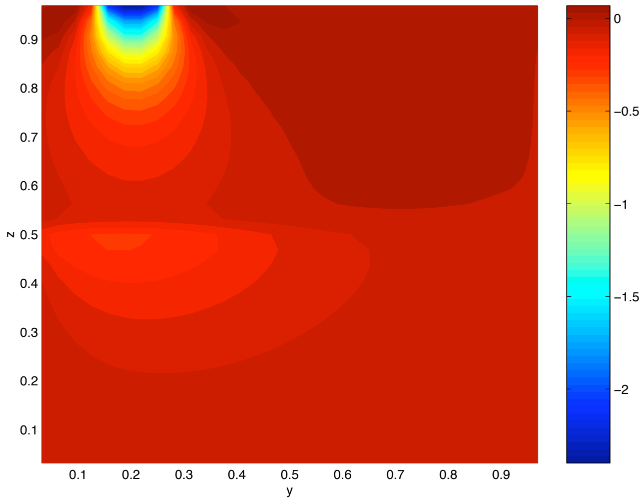

Fig. 9 Example 2: Stress tensor component S^{zz} in the cross-section $x = 0.1875$

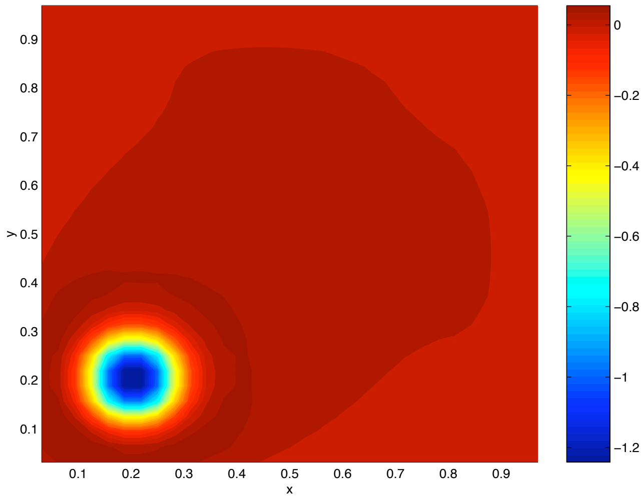

Fig. 11 Example 2: Stress tensor component S^{zz} in the cross-section $z = 0.90625$

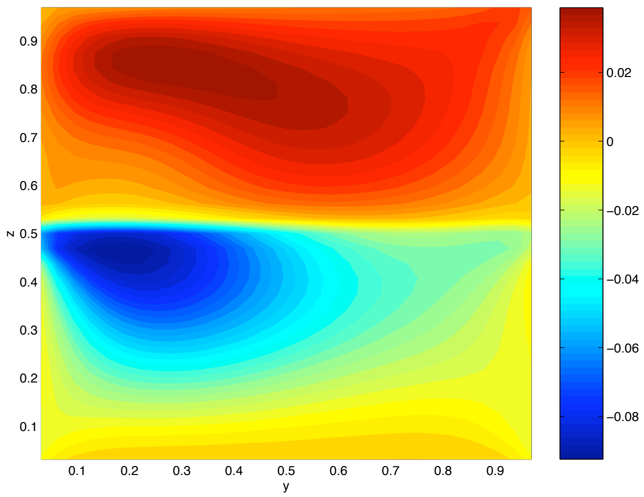

Fig. 10 Example 2: Stress tensor component S^{zz} in the cross-section $x = 0.53125$

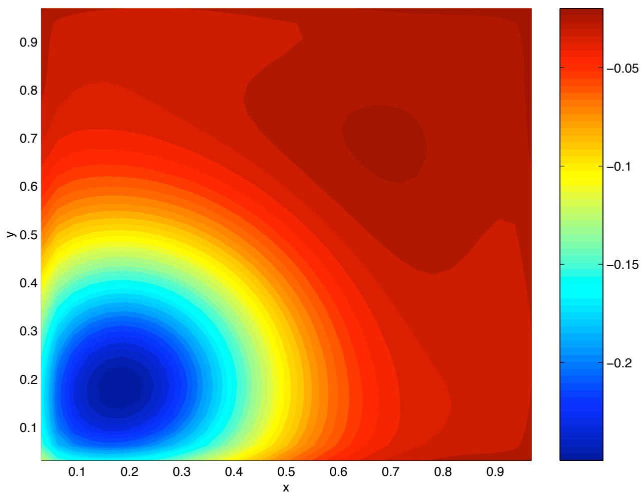

Fig. 12 Example 2: Stress tensor component S^{zz} in the cross-section $z = 0.5$

5. T. Clees, AMG Strategies for PDE systems with applications in Industrial Semiconductor Simulation. *PhD Thesis, Univercity of Köln* (2005).
6. F. J. Gaspar, F. J. Lisbona, and P. N. Vabishchevich, A finite difference analysis of Biot's consolidation model. *Appl. Num. Math.* **44**, 487–506 (2003).
7. F. J. Gaspar, F. J. Lisbona, C. W. Oosterlee, and R. Wienands, A systematic comparison of coupled and distributive smoothing in multigrid for the poroelasticity system. *Num. Lin. Algebra Appl.* **11**, 93–113 (2004).
8. M. Griebel, D. Oeltz, M. A. Schweitzer, An algebraic multigrid method for linear elasticity, *SIAM J.Sci.Comput.* **25**, No.2, 385-407 (2003).
9. S. Knapek, Matrix-dependent multigrid homogenization for diffusion problems., *SIAM J.Sci.Comput.* **20**, No.2, 515-533 (1998).
10. A. A. Samarskii, Theory of difference schemes, Pure and Applied Mathematics, Marcel Dekker, New York, 2001.
11. R.E. Showalter, Diffusion in poro-elastic media, Jour. Math. Anal. Appl., **251**, 310–340 (2000).
12. U. Trottenberg, C. W. Oosterlee, and A. Schüller, Multigrid. Academic Press, New York (2001).
13. R. Wienands, F.J. Gaspar, F.J. Lisbona and C.W. Oosterlee, An efficient multigrid solver based on distributive smoothing for poroelasticity equations. *Computing* **73** 99–119 (2004).
14. P. M. De Zeeuw, Matrix-dependent prolongations and restrictions in a blackbox multigrid solver, *J. Comput. Appl. Math.*, **33**, 1-27 (1990)